Fig. S1

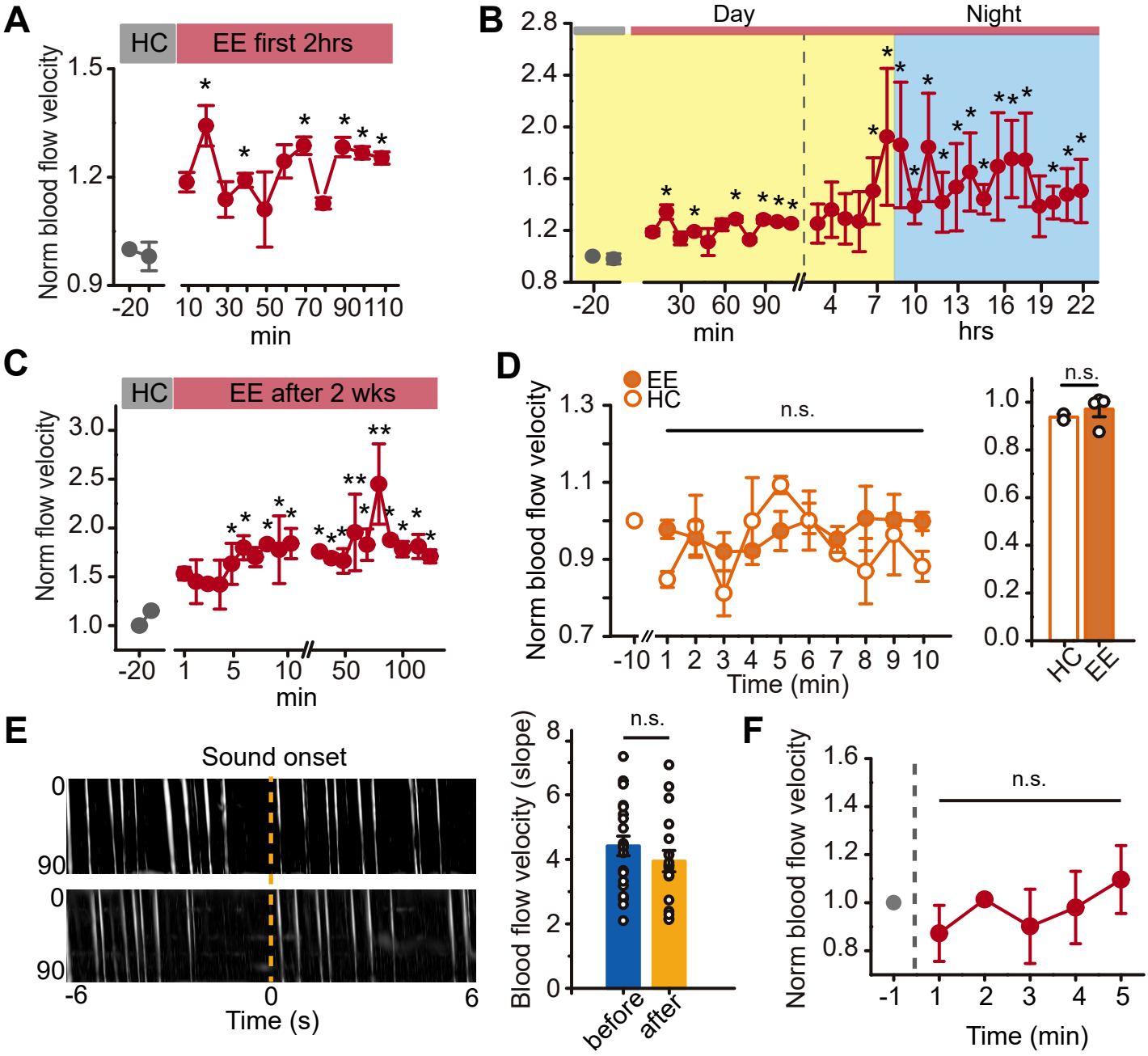

Fig. S1 Hemodynamics in the dentate gyrus during long-term EE exploration and non hippocampus-dependent behavior (related to Fig. 1E & F)

A. Normalized blood flow velocity of the first 2 h of EE exploration (n = 3, Kruskal-Wallis test was used to estimate the differences between later time points and time at -10, * $P < 0.05$).

B. Blood flow velocity in EE for 24 h. Dashed line separates the first 2 h of recording, with 1 min per 10 min and the rest of the recording with 1 min per hour. Shading divides the day and night period. Statistical analysis was the same as that in A.

C. Blood flow velocity in the dentate gyrus on day 14 of EE exposure (1.5 h per day, the combination/location of the object in the EE was changed daily) (n = 2, Linear mixed model for longitudinal data was used to estimate the differences between later time points and time at -10. * $P < 0.05$, ** $P < 0.05/20 = 0.0025$ after Bonferroni adjustment).

D.Blood flow velocity recorded in the auditory cortex during the mice were in HC or EE for 10 min (n = 4 mice for EE and n = 2 for HC, same analysis as in **C**, n.s. $P > 0.05$; the average blood flow velocity in each animal is shown for the bar plot, Wilcoxon signed-rank test was performed using data from all time points, n.s. $P > 0.05$.

E-F. Blood flow velocity recorded in the dentate gyrus during an auditory stimulation. **E**, Sample DMap of blood flow velocity aligned to sound onset (right) and velocity 1 second before or after sound onset (n = 2, each dot represents a velocity value detected, Mann-Whitney test, n.s. $P > 0.05$). **F**, normalized blood flow velocity 1 min before auditory session started (in the same environment) and 5 min of stimulus session (n = 2, similar analysis as in **C**, n.s. $P > 0.05$).

Fig. S2

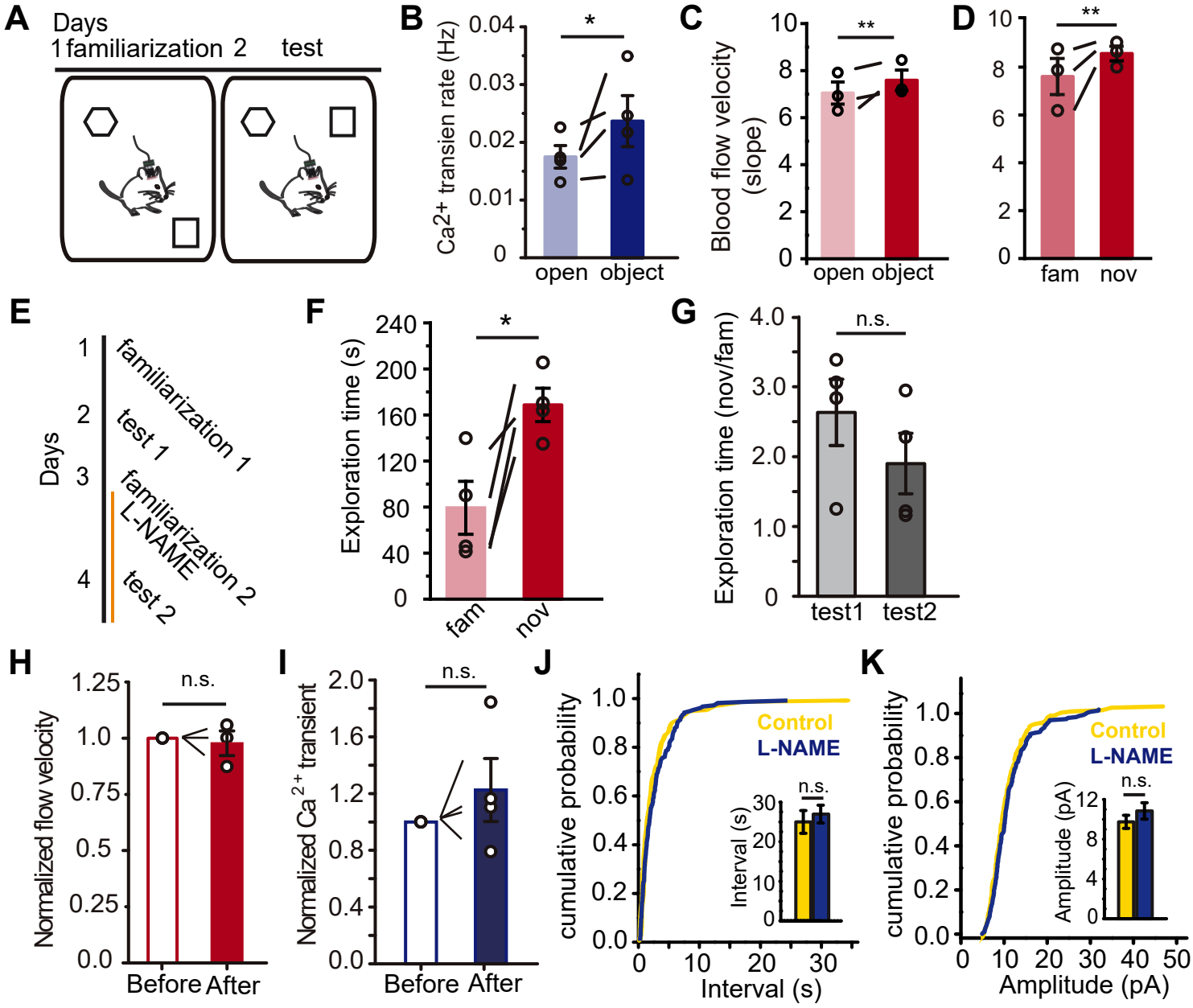

Fig. S2 L-NAME adimistration exhibited minimal effects on behavior and DGC activity (related to Fig. 2C & D).

A. Schematic of novel location recognition task procedure

B. Ca2+ transient rate in the open zone and object zones (n = 4 tests, Ca^{2+} transient rate in all cells was used for statistical analysis but only mean values from each test were shown on the plot, paired Student's t-test, * $P < 0.05$).

C. Blood flow velocity in open and object zones (n = 3, each circle represents the averaged blood flow velocity in each mouse, all velocity values were used for statistical analysis, paired Student's t-test, ** $P < 0.01$).

D. Blood flow velocity in the familiar and novel location zones on test day (n = 3, same analysis as **C**, ** $P < 0.01$).

E. Experimental timeline for evaluating the effect of L-NAME on novel location recognition.

F. Exploration time in familiar and novel location zones on test 2 (n = 4, Kruskal-Wallis test, * $P < 0.05$).

G. Fold change in exploration time in the novel location zone over the familiar object zone on test 1 (before L-NAME) and test 2 (after L-NAME) day (n = 4, Kruskal-Wallis test, n.s. $P > 0.05$).

H. Blood flow velocity 1 d before and after L-NAME administration in HC (n = 3, raw blood flow velocity was used for statistical analysis, Kruskal-Wallis test, n.s. $P > 0.05$).

I. Ca^{2+} transient rate 1 d before and after L-NAME administration in HC (n = 3, same analysis as H, n.s. $P > 0.05$).

J. The cumulative probability of the inter-event interval of miniature excitatory postsynaptic currents (mEPSCs) in DGCs; insert: Quantification of the mEPSC inter-event interval in the control and L-NAME conditions (Control: n = 8 cells; L-NAME: n = 10 cells, Kolmogorov–Smirnov test, n.s., $P > 0.05$).

K. The cumulative probability of the mEPSC amplitude in DGCs(Control: n = 8 cells; L-NAME: n = 10 cells, Kolmogorov–Smirnov test, n.s., $P > 0.05$).

Fig. S3

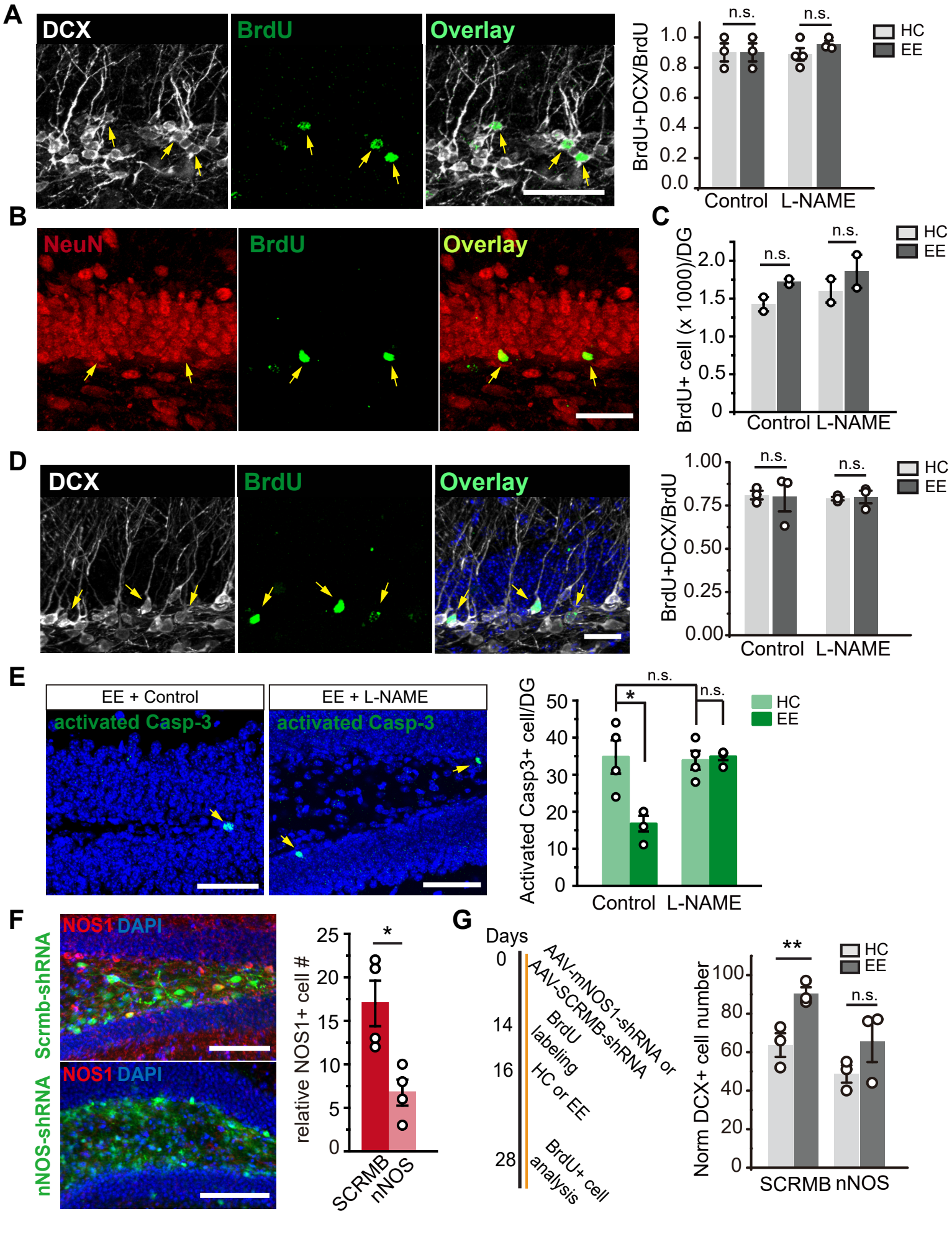
A
DCX
BrdU
Overlay
BrdU+DCX/BrdU
n.s.
n.s.
HC
EE
Control
L-NAME
B
NeuN
BrdU
Overlay
C
BrdU+ cell (x 1000)/DG
D
DCX
BrdU
Overlay
BrdU+DCX/BrdU
E
EE + Control
EE + L-NAME
activated Casp-3
Activated Casp3+ cell/DG
*
F
NOS1 DAPI
Scrmb-shRNA
nNOS-shRNA
relative NOS1+ cell #
SCRMB
nNOS
G
Days
0
14
16
28
AAV-mNOS1-shRNA or AAV-SCRMB-shRNA
BrdU labeling
HC or EE
BrdU+ cell analysis
Norm DCX+ cell number
**

Fig. 3S NO signaling in adult hippocampal neurogenesis (related to Fig. 2E & F)

A. Left, representative confocal images of BrdU and DCX colocalization in the dentate gyrus 14 d after BrdU delivery (silver: DCX, green: BrdU, scale bar: 100 μm). Right, the ratio of BrdU and DCX colocalization did not differ across the four conditions. HC with water (n = 3) or L-NAME-containing water (n = 4) and EE with water (n = 3) or L-NAME-containing water (n = 3) (two-way ANOVA followed by Bonferroni post hoc test, n.s. $P > 0.05$).
B. Representative confocal images of BrdU and NeuN colocalization in the dentate gyrus 14 d after BrdU delivery (red: NeuN, green: BrdU, scale bar: 40 μm).
C. Quantification of the average number of BrdU+ cells in the dentate gyrus at 4 days post BrdU administration for every condition (n = 4, n.s., Two-Way ANOVA followed by Bonferroni post hoc test, n.s., $P > 0.05$).
D. Left, representative confocal images of BrdU and DCX colocalization in the dentate gyrus 4 d after BrdU delivery (silver: DCX, green: BrdU, scale bar: 20 μm). Right, the ratio of BrdU and DCX colocalization did not differ across the four conditions. HC with water (n = 3) or L-NAME-containing water (n = 4) and EE with water (n = 3) or L-NAME-containing water (n = 3), two-way ANOVA with Bonferroni post hoc test, n.s. $P > 0.05$).
E. Left, representative confocal images of activated caspase-3+ cells in the dentate gyrus from EE and EE with L-NAME (green: activated caspase-3, blue: DAPI, brain sections from Fig. 2E). Right, quantification of activated caspase-3+ cells in the dentate gyrus under the four conditions from Fig. 2E. (n = 4 for each condition, Two-Way ANOVA followed by Bonferroni post hoc test, * $P < 0.05$, n.s., $P > 0.05$).
F. NOS1 knockdown efficiency, confocal images of nNOS immunofluorescent labeling in nNOS-shRNA- or scramble-shRNA-injected mice (red: NOS1, green: GFP-shRNA, blue: DAPI, scale bar: 100 μm). Right, quantification of NOS1 fluorescence intensity in each condition (n = 4, Kruskal-Wallis test, * $P < 0.05$).
G. Experimental design timeline evaluating the effect of NOS1-shRNA knockdown on newborn neuron survival. Right, quantification of DCX+ cells in each condition (n = 3, two-way ANOVA with Bonferroni post hoc test, ** $P < 0.01$ n.s. $P > 0.05$).

Fig. S4

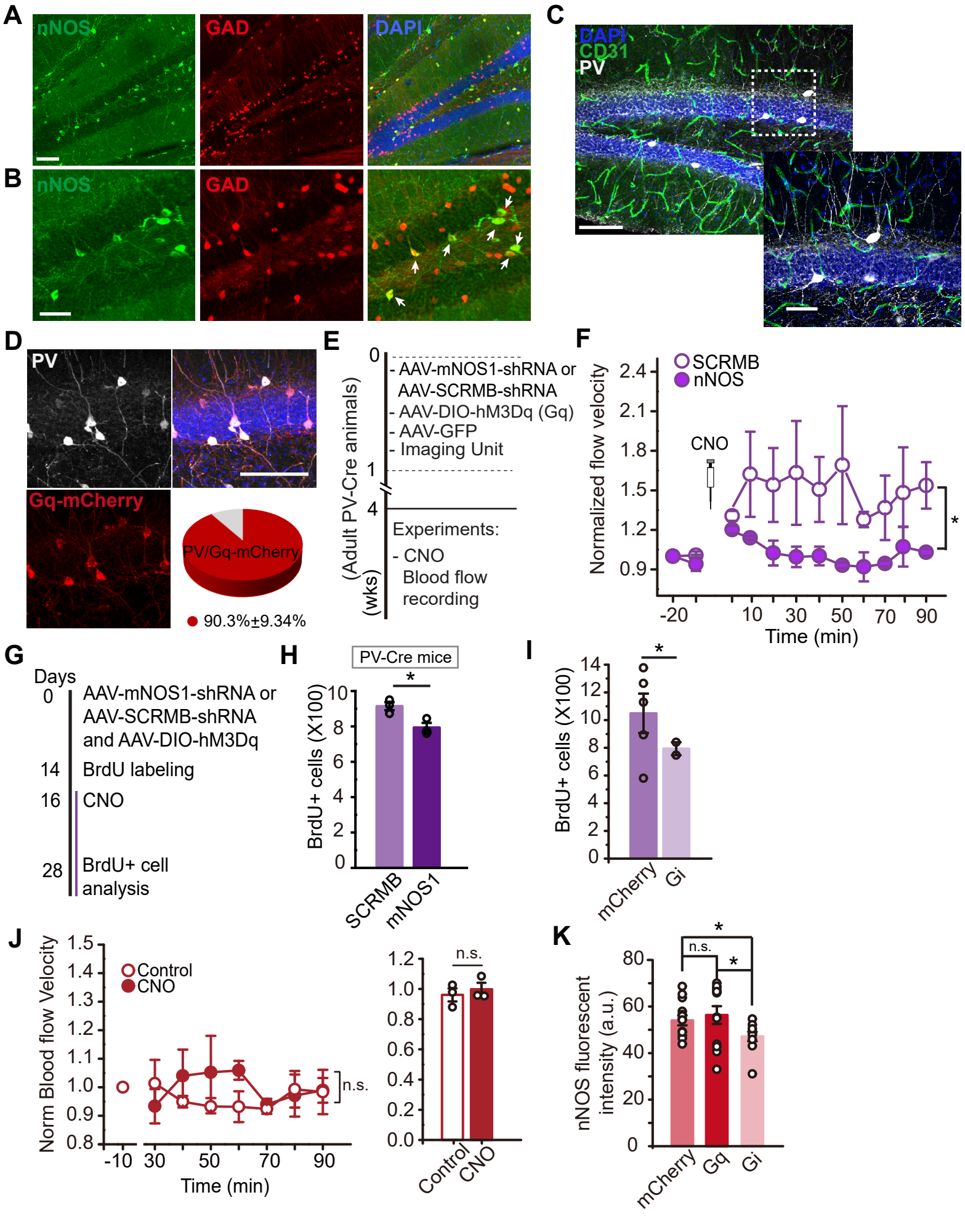
A
nNOS
GAD
DAPI
B
nNOS
GAD
C
DAPI
CD31
PV
D
PV
Gq-mCherry
PV/Gq-mCherry
90.3%±9.34%
E
(Adult PV-Cre animals)
(wks)
0
- AAV-mNOS1-shRNA or
AAV-SCRMB-shRNA
- AAV-DIO-hM3Dq (Gq)
- AAV-GFP
- Imaging Unit
1
4
Experiments:
- CNO
Blood flow
recording
F
SCRMB
nNOS
CNO
Normalized flow velocity
Time (min)
G
Days
0 AAV-mNOS1-shRNA or
AAV-SCRMB-shRNA
and AAV-DIO-hM3Dq
14 BrdU labeling
16 CNO
28 BrdU+ cell
analysis
H
PV-Cre mice
BrdU+ cells (X100)
SCRMB
mNOS1
I
BrdU+ cells (X100)
mCherry
Gi
J
Control
CNO
Norm Blood flow Velocity
Time (min)
n.s.
Control
CNO
K
nNOS fluorescent
intensity (a.u.)
n.s.
mCherry
Gq
Gi

Fig. S4 The role of NO signaling in PV+ neuron mediated hyperemia and neurogenesis (related to Fig. 3)

A. Confocal images of NOS1 (green) expression in the dentate gyrus in a GAD-Cre::tdTomato (red) animal (scale bar: 100 μm).
B. Enlarged confocal images of NOS1 and GAD2 colocalization in the sub-granular zone (scale bar: 50 μm).
C. Confocal images of PV+ neurons and vasculature in the dentate gyrus (blue: DAPI; green: CD31; silver: PV, scale bar: 100 μm). The image on the right is an enlarged area from the dashed box (scale bar: 50 μm).
D. Confocal images of the colocalization of PV+ neurons with AAV-DIO-Gq-mCherry in the dentate granule cell layer from PV-Cre animals (n = 6, silver: PV, red: mCherry, blue: DAPI, 90.3% ± 9.34% of PV+ neurons were labeled by AAV, scale bar: 100 μm. Enlarged image scale bar: 50 μm)
E. Experimental timeline of blood flow imaging following nNOS knockdown in PV-Cre mice.
F. Normalized blood flow velocity in PV-Cre mice with scramble-shRNA (control) and NOS1-shRNA knockdown (n = 2 , the value from all time point in each animal was used for statistical analysis, Kruskal-Wallis test, * $P < 0.05$).
G. Experimental design of newborn neuron survival in nNOS knockdown the PV-Cre mice.
H. Quantification of BrdU+ cells in PV-Cre mice with scramble or NOS1-shRNA in the dentate gyrus (n = 3, Kruskal-Wallis test, ** $P < 0.01$).
I. Quantification of BrdU+ cells in PV-Cre mice injected with AAV-DIO-mCherry (n = 4) or –hM4Di (n = 2) in the dentate gyrus (Kruskal-Wallis test, * $P < 0.05$).
J. Left: Normalized blood flow velocity in mice injected with GFP only (no DREADDs) in the dentate gyrus pre- and post-saline or CNO administration (n = 3, Linear mixed model for longitudinal data was used to estimate the differences between saline and CNO at each time point. n.s. $P > 0.05$). Right: Quantification of the average blood flow velocity in each condition (n = 3, Wilcoxon signed-rank test was performed using data from all time points, n.s. $P > 0.05$).
K. Quantification of NOS1 fluorescence intensity in PV-Cre mice injected with AAV-DIO-mCherry, -hM3Dq, or

Fig. S5

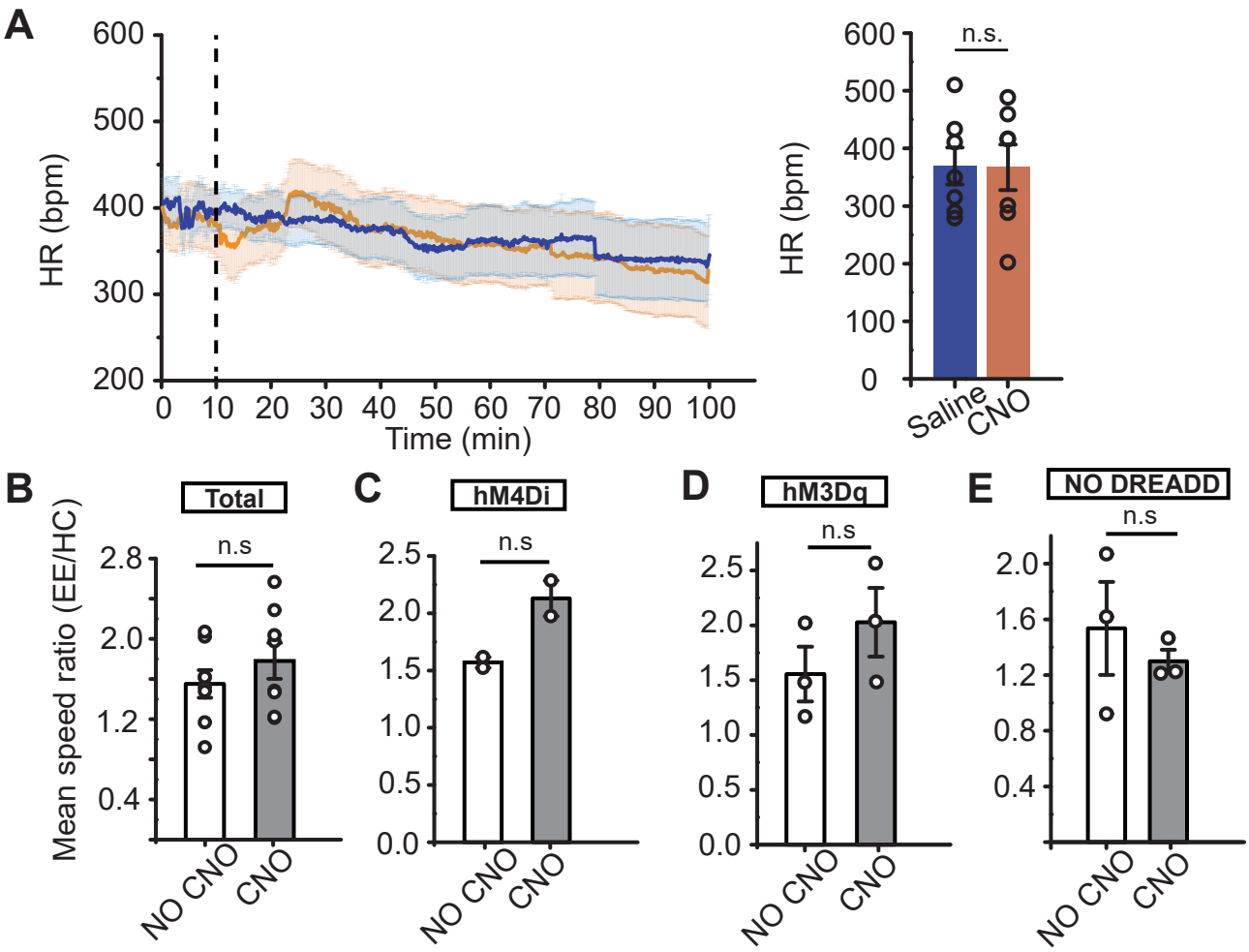

Fig. S5 The manipulation of DGCs with DREADD exhibited minial effects on physicological condtions (related to Fig. 4 & 5)

A. Mice heart rates were recorded for the bidirectional manipulation (Fig. 4). Left: Heart rate throughout the recording sessions. The dashed line indicates the saline or CNO intraperitoneal injections. Right: Quantification of the average heart rate in each recording condition (n = 7, paired Student's t-test, n.s., P > 0.05).

B-E. CNO did not affect locomotion in the EE. **B**. The EE/HC ratio of total distance in all animals with or without CNO (n = 8, paired Student's t-test, n.s., P > 0.05). **C**. The EE/HC ratio of total distance in animals injected with Gi with or without CNO (n = 2, paired Student's t-test, n.s., P > 0.05). **D**. The EE/HC ratio of total distance in animals injected with Gq with or without CNO (n = 3, paired Student's t-test, n.s., P > 0.05). **E**. The EE/HC ratio of total distance in animals lacking DREADDs with or without CNO (n = 3, paired Student's t-test, n.s., P > 0.05).

F. Confocal images of DCX+ cells and AAV-CaMKII-Gq-mCherry (red: Gq-mcherry, green: DCX, blue: DAPI, scale bar: 20 μm).

Fig. S6

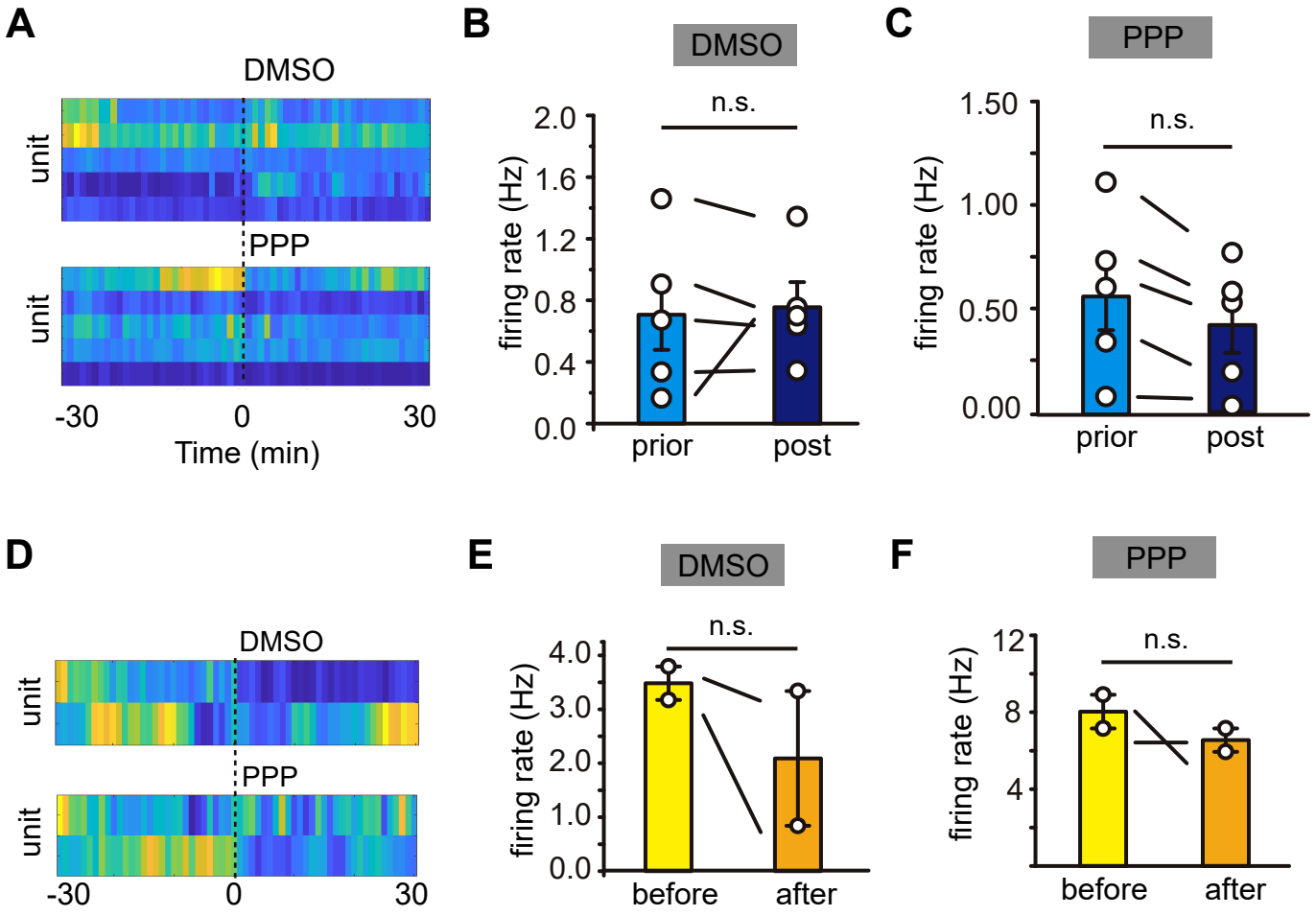

Figure S6 PPP local infusion did not alter the neuronal activity in the dentate gyrus (related to Fig. 6)
A. Color map of in vivo electrophysiology recordings of DGCs pre- and post-DMSO/PPP administration.
B. Quantification of DGC firing rate pre- and post-DMSO infusion (n = 5, Wilcoxon signed-rank test, n.s., P > 0.05).
C. Quantification of DGC firing rate pre- and post-PPP infusion (n = 5, Wilcoxon signed-rank test, n.s., P > 0.05).
D. Color map of in vivo electrophysiology interneuron recordings pre- and post-DMSO/PPP administration.
E. Quantification of DGC firing rate pre- and post-DMSO infusion (n = 2 cells, Wilcoxon signed-rank test, n.s., P > 0.05).
F. Quantification of DGC firing rate pre- and post-PPP infusion (n = 2 cells, Wilcoxon signed-rank test, n.s., P > 0.05).